JOURNAL OF AIRCRAFT
Vol. 29, No. 4, July–Aug. 1992

Flight Model for Unmanned Simulated Helicopters

Amnon Katz*
University of Alabama, Tuscaloosa, Alabama 35487
and
Brett E. Butler†
McDonnell Douglas Helicopter Company, Mesa, Arizona 85205

This paper presents a flight model for use in simulating computer generated helicopters. Momentum and energy balance is used to define a rotor thrust envelope. The four basic control inputs take the form of thrust components and the sideslip angle. Time integrations are performed for the three center of mass degrees of freedom only. Six degrees of freedom information is derived for the visual displays. The model can inexpensively function in real time and faster than real time. Validity is demonstrated by comparing model performance predictions with published data.

I. Introduction

THE flight models used in manned simulation must respond correctly to control inputs made through authentic aircraft controls. The pilots flying the simulator expect to experience all secondary control effects such as adverse yaw and p-factor, in the case of fixed-wing propeller-driven aircraft. The requirements for computer generated aircraft flying interactively within the manned simulation are quite different. These aircraft merely have to appear realistic and indistinguishable from manned aircraft to the pilots viewing them from the outside.

In the case of computer generated aircraft, secondary control effects are irrelevant. What is simulated here is the combination of an aircraft and its competent pilot. The pilot compensates for the secondary effects to a point where they are unobservable. All that needs be simulated is correct performance.

It is not an unreasonable approximation to assume that competent pilots can control the attitude of their aircraft at will, subject only to rate limitations that are easily implemented without a dynamical model. Similarly the power output can be controlled practically at will, and a detailed engine model is not required. But the computer generated aircraft is still subject to basic point-mass dynamics. It cannot get from one point to another without an appropriate velocity maintained over a period of time. And velocity cannot be changed without generating the forces that give rise to the required acceleration.

These considerations suggest a simplified flight model: Attitude and power are controlled directly (subject to ad-hoc limitations). From these the loads are derived, which are then used to integrate the 3 degrees of freedom of center of mass motion. Only these three are treated as dynamic degrees of freedom. One might refer to this type of model as a 3-degrees-of-freedom flight model. (However, this nomenclature is not universal, and a similar model might be called a 6-DOF model because 6-DOF information is derived.)

Simplification suggests itself also in the area of control inputs. For unmanned simulation it is not necessary for control inputs to be in the form of stick, rudder, and throttle, or of cyclic, pedals, and collective. It suffices to have four independent primary control inputs, which are chosen for ease of computing both attitudes and loads. The attitude itself can be used: e.g., heading, pitch, bank, and power level. But variables related to the air velocity vector are more relevant for computing loads. A very handy set of control variables for fixed-wing aircraft is: angle of attack, bank, power, and angle of sideslip. The last input is maintained at zero for coordinated flight. In this way, while all 3-DOF flight models treat only the center of mass motion by time integration of dynamic equations, they differ in the choice of the four primary control inputs and in the equations through which attitude and loads are determined.

Austin et al.[1] implemented a real-time and faster-than-real-time mechanization of an unmanned helicopter along these lines. They obtain forces from tables of achievable loads that are maneuver specific. This limitation precludes the arbitrary application of control inputs, and in this sense the scheme of Ref. 1 does not constitute a flight model. Also, the tables, which are model specific, may not be readily obtainable.

In the present paper we develop a 3-dynamic-degrees-of-freedom (6-output-degrees-of-freedom) flight model for computer generated helicopters. The model is intended for implementation of computer generated autonomous combat helicopters[2]—the same type of application as addressed by Austin et al. The selection of dynamic degrees of freedom and of control inputs is also similar to Ref. 1. However, the computation of forces is based neither on details of rotor mechanics, nor on table lookup methods, but rather on the basic physical ideas of the so-called momentum theory. This approach achieves extreme simplicity and efficiency. Our model is suitable for applications that run in real time and faster than real time. In the alternate, our computations might be used to produce tables such as used by Austin et al. We require only one specific parameter.

The control inputs we select are the three components of rotor thrust and the fuselage sideslip angle. (For coordinated flight this last input vanishes.) We allow the simulated pilot to manipulate rotor thrust at will subject to certain ad hoc rate limitations and to performance limits derived from the basic physical principles of conservation of momentum and energy (momentum theory). The cost of generating the desired thrust is estimated in terms of power required. The "pilot" is constrained not to exceed the power available. Note that this does not preclude transient maneuvers that draw on the aircraft's kinetic energy, but merely enforces conservation of energy (see Sec. III.B.3). Other flight restrictions (e.g., based on rotor maximum thrust capability and on static or dynamic structural considerations) may apply as well.

Received Dec. 10, 1990; revision received May 17, 1991; accepted for publication May 27, 1991.

*Professor, Department of Aerospace Engineering. Member AIAA.
†Member Technical Staff.

Put another way, the model defines a thrust envelope made up of the union of surfaces corresponding to maximum power and minimum power. This envelope may be further restricted by surfaces reflecting other (aerodynamic, structural, or operational) limitations. The "pilot" is free to select any thrust vector within the envelope or on it. A thrust vector on the envelope goes with an extreme maneuver. Maneuvers using a thrust vector inside the envelope may be called moderate.

The result is an economical and elegant model that takes little space and time to state, to analyze, to implement, and to execute. The model is also reasonably accurate when compared to flight test data.

The physical basis of the model is given in Sec. II. Section III illustrates the method of applying the performance limitations. Section IV offers comparison of predicted performance limitations to published data. Section V outlines the flow of the flight model. Section VI is a summary. Details of computation algorithms are presented in the Appendix.

II. Power Required to Produce Thrust

We decompose the thrust $\boldsymbol{T}$ into a longitudinal component, T_L, along the velocity and a transverse component, T_T, perpendicular to it (Fig. 1). The velocity in question, $\boldsymbol{V}$, is that of the motion of the aircraft relative to the air mass. (Boldface letters are used for vectors and the same normal letter denotes the magnitude of the vector.) The decomposition of a vector into longitudinal and transverse components takes place in the plane defined by the velocity vector, $\boldsymbol{V}$, and the thrust vector, $\boldsymbol{T}$. It bears no relationship to horizontal and vertical. The weight vector, $\boldsymbol{W}$, in Fig. 1 may point in any direction or even out of the plane of the figure depending on the helicopter's attitude.

The importance of the distinction between longitudinal and transverse is that in translational flight the longitudinal thrust performs work, while the transverse thrust does not. Power available limitations therefore impose much stricter limits on T_L than on T_T. While a transverse load factor of say, 2, can be sustained by most helicopters in translational flight, nothing of the kind can be achieved in the direction of flight. The distinction between longitudinal and transverse fades at low speeds and is lost in hover.

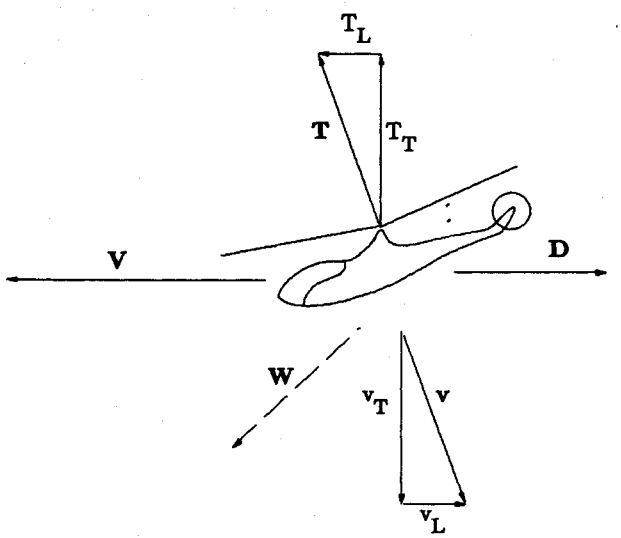

Fig. 1 Notations. The plane of the figure is the one containing V—the velocity of the helicopter relative to the airmass and the rotor thrust T. The thrust T and the rotor induced velocity v are decomposed into longitudinal components along V and transverse components perpendicular to it. The weight W can point in any direction, including out of the plane of the figure.

The power expended as work done by longitudinal thrust may be represented as

$$P_0 = \boldsymbol{T}\cdot\boldsymbol{V} = T_L V \tag{1}$$

by definition of the component T_L.

However, the production of thrust in any direction is not without a cost in power. The rotor "pushes" on air to obtain its thrust. The air is set in motion in the process and acquires kinetic energy that must be supplied. Let us denote the mass of air affected per unit of time M and the added velocity it acquires v. Then Newton's second law dictates

$$\boldsymbol{T} = M\boldsymbol{v} \tag{2}$$

The power absorbed is

$$P_1 = \tfrac{1}{2}Mv^2 = \tfrac{1}{2}\boldsymbol{T}\cdot\boldsymbol{v} \tag{3}$$

In the following v, too, is decomposed into longitudinal and transverse components (Fig. 1).

We now proceed to estimate M. We start by addressing two extreme cases: hover and fast translational motion. In hover we call upon classic actuator disk theory.[3] The speed of flow through the actuator disk is half the final slipstream speed, and therefore the rate of mass flow is

$$M = \tfrac{1}{2}\rho\pi r^2 v \tag{4}$$

where ρ is air density and r is the rotor radius. In the other extreme case we draw on the classical theory of induced drag due to Munk.[4] In transverse view, the rotor disk is like a flat circular plate "pushing" on the airstream. The affected mass is the "added mass" of a flat plate, which amounts to a circular cylinder of air with radius equal to the rotor radius:

$$M = \rho\pi r^2 V \tag{5}$$

In either case the mass is obtained as the flow per unit time through an area equal to the rotor area and placed at the rotor perpendicular to the flow. Putting the two extreme cases together, one postulates that the same rule for obtaining the effective mass flow holds also in all intermediate cases:

$$M = \rho\pi r^2|V + \tfrac{1}{2}v| = \rho\pi r^2(V^2 + \tfrac{1}{4}v^2 + Vv_L)^{1/2} \tag{6}$$

This assumption was first made by Glauert in 1926 in the context of the autogiro.[5] See Ref. 6 for a modern account of momentum theory.

The total power required to produce thrust T is the sum of Eqs. (1) and (3):

$$P = T_L V + \tfrac{1}{2}\boldsymbol{T}\cdot\boldsymbol{v} = T_L(V + \tfrac{1}{2}v_L) + \tfrac{1}{2}T_T v_T \tag{7}$$

In Eqs. (6) and (7) the subscripts L and T applied to any vector denote components along and across the aircraft velocity. Next eliminate the components of v from Eqs. (7) and (6) by substituting their values from Eq. (2). This yields

$$P = T_L V + \tfrac{1}{2}T^2/M \tag{8}$$

$$M = \rho\pi r^2[(V + \tfrac{1}{2}T_L/M)^2 + \tfrac{1}{4}T_T^2/M^2]^{1/2} \tag{9}$$

Equations (8) and (9) together define the power required to produce thrust $\boldsymbol{T}$. One would like to eliminate M between the last two equations to obtain power in terms of thrust alone. This cannot be done in closed form, because the equations are quartic in M. However, useful approximations and efficient iteration schemes are available for solving for P in terms of T. These are discussed in the Appendix.

The power P in Eq. (8) is ideal thrust horsepower which neglects all losses due to form drag of rotor blades, eddy

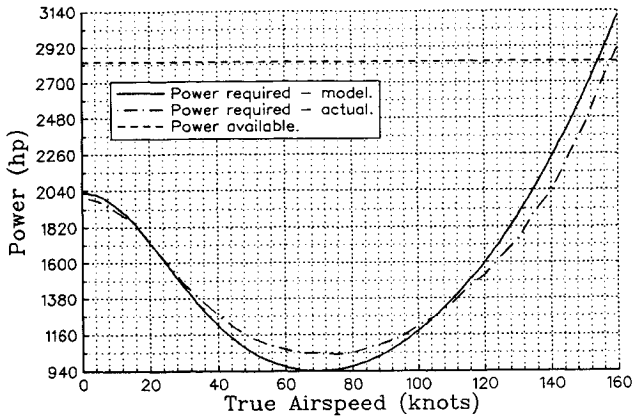

Fig. 2 Power required. Model prediction and published data for the AH-64 Apache.

motion in wakes, and power expended by the anti torque system. We relate it to engine shaft horse power P_s by

$$P = KP_s \tag{10}$$

where K is an efficiency factor smaller than one. We find in Sec. IV that a constant K, independent of T and V, affords adequate representation of test results (Fig. 2).

III. Thrust Envelope

Equations (8) and (9) may be used to solve for P, given T. Alternately, they may be viewed as defining the thrust locus for given P. The thrust loci for the maximum power, P_{max}, and the minimum power, P_{min}, together form the thrust envelope. Any thrust within the envelope or on it may be realized by proper power setting and control application. Thrust vectors that fall outside the envelope are unachievable.

The concept of the thrust envelope naturally leads to the distinction between moderate maneuvers and extreme maneuvers.

A. Moderate Maneuvers—Solving for P

For the purpose of the present discussion, a moderate maneuver is one that uses a thrust vector inside the envelope. It is performed at an intermediate power level, below the maximum available power and above the minimum. Moderate maneuvers include straight and level flight below maximum speed, gentle turns, climbs, descents, and combinations thereof.

For moderate maneuvers, the role of the present flight model is limited to verifying that the maneuver is indeed moderate. The desired components of thrust are determined. The power required is computed to verify that it does indeed fall between the upper and lower limits of its range. The thrust components are then used in the equations of motion of the center of mass.

B. Extreme Maneuvers—Solving for T

Extreme maneuvers are defined for our purpose as ones that require a thrust vector on the thrust envelope. For an extreme maneuver the power is set at an extreme point of its range. Maximum performance accelerations, decelerations, climbs, and turns are extreme maneuvers. The class of extreme maneuvers includes several subclasses.

1. Extreme Sustained Transverse Maneuvers

These maneuvers are those extreme maneuvers in which it is desired to make the transverse thrust as high as possible while achieving or maintaining a desired steady state. The longitudinal component of thrust is set to balance drag at the desired speed. Maximum performance sustained level turns at a constant airspeed can illustrate this case, with T_L set equal to the drag at the speed in question. (See Sec. III.B.3 below for transient transverse maneuvers.)

The procedure to compute the thrust for an extreme transverse maneuver is as follows: The required T_L and $P = P_{max}$ are substituted in Eq. (8) which is then solved for the transverse thrust

$$T_T = \{2M[P_{max} - T_L V - T_L^2/(2M)]\}^{1/2} \tag{11}$$

This is the maximum absolute value of the transverse thrust, that may be applied in any transverse direction. In the case of the sustained level turn, it is applied so that its vertical component is equal to the weight of the aircraft.

Before an envelope of transverse thrust vs speed can be obtained, the mass rate M must be eliminated between Eqs. (9) and (11). Approximations and iteration schemes for this purpose are discussed in the Appendix. See Fig. 3 for a computed envelope of transverse thrust vs airspeed. (The thrust in Figs. 3, 4, and 5 is normalized to the aircraft gross weight W. What is plotted is the load factor T/W.)

2. Extreme Longitudinal Maneuvers

These are extreme maneuvers in which the transverse components of thrust are set to moderate values and the power is pushed to the limit of its range in an attempt to maximize or minimize the longitudinal thrust. Maximum performance straight and level acceleration and deceleration may serve to illustrate this class, with T_T set equal to the weight of the aircraft.

We now substitute the appropriate T_T and P in Eq. (8) and solve for T_L

$$T_L = -MV \pm (M^2V^2 + 2MP - T_T^2)^{1/2} \tag{12}$$

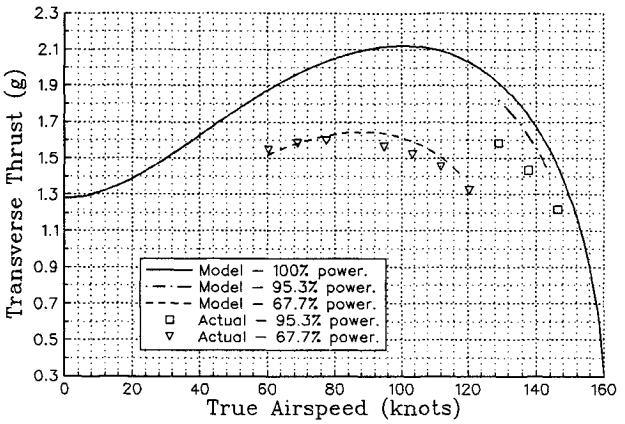

Fig. 3 Transverse load envelope. Model prediction and published data for the AH-64 Apache. Model full envelope is for full power. Measured points are for 95.3% power or 67.7% power as marked. Segments of the model predicted curves for these power levels are included for comparison.

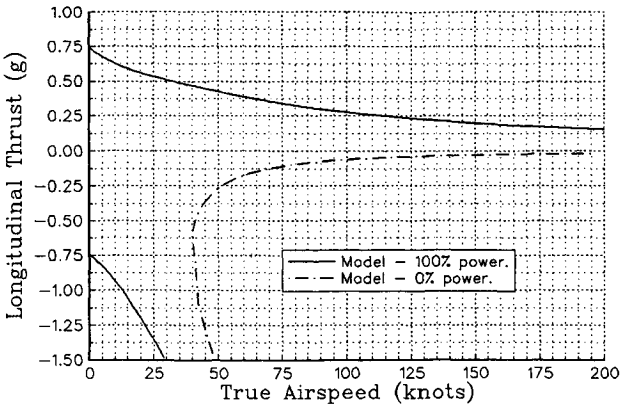

Fig. 4 Longitudinal thrust envelope. Model prediction for the AH-64 Apache.

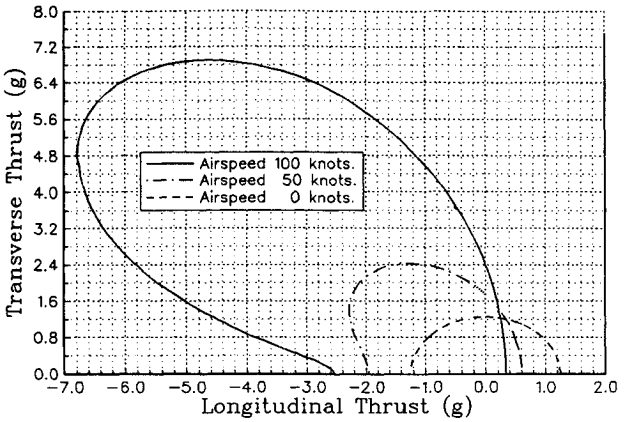

Fig. 5 Thrust vector envelopes. Envelopes of transverse vs longitudinal for selected airspeeds.

The envelope of longitudinal thrust is more complex than its transverse counterpart. For each combination of V and P there either are two values of T_L, or none at all. A complete envelope is shown in Fig. 4. It is made up of the two branches of Eq. (12) for $P = P_{max}$ and the branches for $P = P_{min}$. For approximate or iterative methods of eliminating M between Eq. (12) and Eq. (8) again see the Appendix.

The envelope of Fig. 4 is based on maintaining a transverse load of 1 g. The top branch of the envelope represents the use of all available power to maximize forward thrust. The next curve down represents the use of minimum power. Energy is absorbed from the airstream to produce the transverse 1 g, and the result is negative (backward) longitudinal thrust. (Energy could in principle be drawn from the airstream also to turn the shaft. Absorption of energy by the engine from the rotor is precluded in helicopters as a matter of design. The transmission disengages from the engine when the latter is absorbing energy. But some energy could still be absorbed in the transmission and tail rotor. We neglect these effects here for lack of sufficient data.) The bend in this part of the envelope signals the lowest speed at which 1 g can be maintained without power. At higher speeds 1 g can be maintained two ways: at a moderate pitch with moderate thrust or at a high pitch with higher thrust. The latter represents higher values of backward thrust. Such values may be further increased by application of power to produce rearward thrust as represented by the lowest part of the envelope.

3. Other Extreme Maneuvers

Extreme maneuvers are by no means confined to sustained transverse and longitudinal. Other extreme maneuvers include the transient extreme transverse maneuver in which the transverse thrust is set as high as possible for the momentary speed. An emergency pullup aimed at maximizing the vertical component of thrust is a transient extreme maneuver that is neither transverse nor longitudinal. For the purpose of these maneuvers one would study Fig. 5 which shows the T_T vs T_L envelopes for given V. For the extreme transient transverse maneuver one would look for the highest point on the curve. This curve entails a negative longitudinal thrust component—absorbing energy from the airflow and slowing the helicopter down. In case of the emergency pullup one would look for the point on the envelope where the slope equals the dive angle.

Note that the envelopes shown here are based solely on momentum and energy balance. Envelope restrictions based on structural, aeroelastic, or other operational limitations as well as on more detailed aerodynamic considerations must be superimposed on the thrust envelopes derived here before they are applied.

IV. Validation and Discussion

In this section the validity of the present model is demonstrated by comparing its predictions to published performance data for the McDonnell Douglas AH-64 Apache.[7] The rotor diameter of the Apache is 48 ft. Drag was computed using an equivalent drag area of 35.91 ft^2.[8] The efficiency factor K in Eq. (11) was set to 0.54. For further discussion of data fit and parameter selection see below.

Figure 2 displays the 1 g power required as a function of speed. This is the result of solving Eqs. (8) and (9) for P. The value plotted is P/K. This curve is superimposed on the measured curve obtained from Ref. 7. Both curves are for a primary mission configuration AH-64 at a gross weight of 14,766 lbs.

Figure 3 shows the transverse load envelope. It is the result of solving Eqs. (9) and (11) for T_T, with T_L set equal to the drag at the given speed. The value displayed is T_T/W. Superimposed on this envelope are values of transverse thrust derived from the tables of Ref. 9. The measurements in the reference were made at varying power levels. Points computed for 95.3% power and 67.7% power are shown in Fig. 3 together with prediction of the model for those power levels.

Longitudinal thrust in Fig. 3 is adjusted to offset drag at applicable speed. Both model predictions and Ref. 9 data are based on the same configuration (8 Hellfire missiles), so that the drag is the same. The data were obtained in level flight at different gross weights. The transverse thrust values are shown in Fig. 3 as multiples of 14,766 lbs, to allow direct comparison with model data for that gross weight.

The close agreement of model predictions with the flight test data at moderate load level and speed (the 67.7% points) reflects the soundness of the basic physical asssumptions made. At 95.3% power and higher speed, a systematic difference becomes apparent with the load actually developed being lower than predicted. This is probably due to the retreating blade angle of attack approaching stall—a phenomenon for which the model does not account.

The 95.3% power points, being closer to the thrust envelope, are more representative of the accuracy of model predictions for the envelope than the 67.7% power points. The points shown probably represent the worst case because of the high speed. At lower speeds, asymmetry between advancing and retreating blades is less pronounced, and momentum theory is more accurate.

Figure 4 shows the longitudinal load envelope. Here Eqs. (9) and (12) are solved for T_L, with $T_T = W$, and P set to KP_{smax} for acceleration and to zero for deceleration (see discussion of extreme longitudinal maneuvers in Sec. III). The values shown are T_L/W.

Figure 5 shows the T_T vs T_L envelopes for three values of airspeed V. All figures address a standard day at sea level.

The data in Fig. 2 agrees with the published power required curve[8] to within 10%. By this we mean that each point on the one curve has a corresponding point on the other with root mean square of the percent deviation in values of the abscissa and ordinate not more than 10%. Similar agreement is evident in Fig. 3.

This fit was obtained with just one variable parameter—the efficiency factor K. A somewhat closer fit is possible if the equivalent area, too, is deduced from the fit rather than the literature. (This would result in an equivalent drag area of 32.7 ft^2, an efficiency factor $K = 0.52$, and a fit to within 7.5%.) Even further improvement should be possible by allowing the efficiency factor to depend on speed and other variables. However, such practices complicate the model. Furthermore, any attempt to elaborately fit any one particular curve would deviate from the first-principles basis of the model that assures all around correctness. So long as one stays with the simple one parameter model described in this paper, there is no point in solving the equations of Sec. II and III to an accuracy better than 1%. This is possible in very few iterations, and in many cases (see Appendix) by closed form approximations. All of this leads to a very economical model that can easily be implemented in real time.

V. Flight Model

The function of a simulation flight model is to produce the state variables of the aircraft being simulated based on initial conditions and on control inputs. The current model produces the position and orientation of the simulated helicopter as a rigid body.

Six degrees of freedom may not be adequate to correctly represent a helicopter. Still, even when manned helicopter simulators employing sophisticated flight models are operated interactively, each helicopter is normally presented visually to the pilot of the other as a rigid body. So long as this practice continues, presentation of the unmanned player as rigid will not betray its identity; but unbelievable performance might. It is the performance that is crucial. Reproducing realistic performance inexpensively is the main thrust of the present model.

The model computation follows these steps in each simulation frame:

1) Read the control inputs: thrust vector and fuselage sideslip angle.

2) Condition these variables: a) If commanded thrust direction varies from previous direction by more than rate limits permit, establish actual thrust direction closer to previous direction (optional). b) If magnitude of commanded thrust exceeds envelope, scale actual thrust to lie on the envelope. c. If commanded sideslip angle varies from previous angle by more than rate limits permit, establish actual sideslip angle closer to previous angle (optional).

3) Compute drag based on current airspeed (and optionally on sideslip angle).

4) Use actual thrust, together with weight and drag, to integrate center of mass position.

5) Display helicopter as a rigid model at the new c.g. location, with the rotor disk perpendicular to the thrust vector and the fuselage rotated to the actual sideslip angle.

The control inputs for a computer generated player must come from some "logic engine." In our own application this consists of two stages: A high level decision logic[2] that produces abstract decisions (turn, climb . . .) and a lower level "maneuver interpreter" (MI) that translates these decisions into frame by frame control inputs. The MI will be the subject of a separate paper. In our application the MI itself computed the thrust limits, obviating the need to perform the check of commanded thrust against the thrust envelope as described above.

VI. Conclusions

The requirements for a flight model for a computer generated player in simulation are correct performance and inexpensive execution. Unlike models for manned simulation, handling qualities as such are immaterial. The model described in this paper meets these requirements. Performance is predicted within a few percent. Being based on sound physical principles, the model is flexible enough to cover all flight situations, including transient maneuvers. The model is also fast enough to run in real time and faster than real time in applications such as tree lookahead.

Appendix: Mass Rate M

All of the results quoted in this paper required the elimination of the mass rate M between Eq. (9) and Eq. (8) or a variant thereof. This appendix addresses the computation of M.

We start by treating the two extreme cases of hover and high speed translation. In hover ($V = 0$), Eq. (9) simplifies to the point that M can be obtained in closed form:

$$M_h = [\tfrac{1}{2}\rho\pi r^2(T_L^2 + T_T^2)^{1/2}]^{1/2} \qquad \text{(A1)}$$

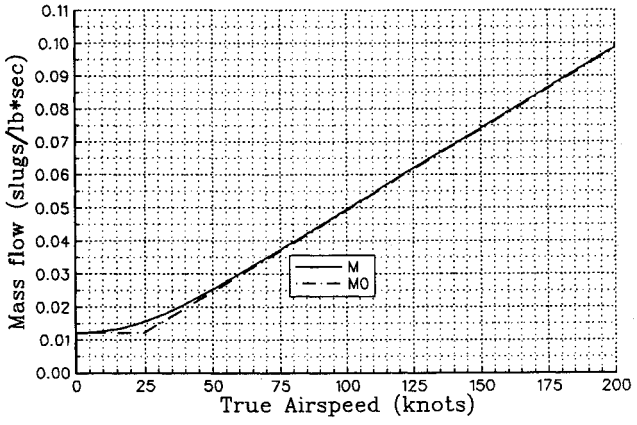

Fig. 6 Mass rate M. Model prediction for the AH-64 Apache (normalized to aircraft gross weight); First Guess M_0 and converged solution.

In high-speed translation, the thrust dependent terms become insignificant, and M reduces to

$$M_t = \rho\pi r^2 V \qquad \text{(A2)}$$

The last equation is identical with Eq. (5) in the body of the paper.

The simplest approximation to M is to use (A1) or (A2), whichever is larger:

$$M_0 = \max(M_h, M_t) \qquad \text{(A3)}$$

At low speeds the constant (A1) is applied. At higher speeds the linear (A2) takes over. This approximation is shown in Fig. 6 together with a numerical solution of Eqs. (8) and (9). It is seen that M_0 affords an excellent approximation to M everywhere except near the bend. There the error reaches about 20%.

It is easy to improve on (A3) by iteration. One starts with M_0 and substitutes it in the right side of Eq. (9) to obtain a new value M_1. One continues in this fashion

$$M_{n+1} = \rho\pi r^2[(V + \tfrac{1}{2}T_L/M_n)^2 + \tfrac{1}{4}T_L^2/M_n^2]^{1/2} \qquad \text{(A4)}$$

until following values of M_n are within the desired tolerance. It takes only three iterations to obtain an accuracy of 1%. (This is the bound on deviations from the true predictions of the current model, which itself may deviate from reality by up to 10% as discussed above.)

When $\boldsymbol{T}$ is not known, and it is desired to maximize or minimize a component of $\boldsymbol{T}$, the iteration scheme becomes more complex. Simultaneous values of M and the unknown component of $\boldsymbol{T}$ are substituted in the right sides of Eqs. (9) and (11) or in Eqs. (9) and (12) as the case may be. The left sides then define the next values of M and the variable component of $\boldsymbol{T}$. The procedure continues until both M and the $\boldsymbol{T}$ component settle within the desired tolerance. Again three iterations are enough to produce 1% accuracy.

Note that the curve of M vs V in Fig. 6 is for cruise at the speed in question. M will vary with the maneuver (the thrust component). Under normal operating practices M is close to that shown in Fig. 6. However on the low branches of the longitudinal thrust envelope of Fig. 4 (the ones shown dashed) M is close to M_h even at speed.

Acknowledgments

The authors wish to thank Frank Okamoto, Perumal Shanthakumaran, and Roger Smith of McDonnell Douglas Helicopter Company for discussions and constructive comments on the draft manuscript.

References

[1]Austin, F., Carbone, G., Falco, M., and Hinz, H., "Automated Maneuvering Decisions for Air-to-Air Combat," Grumman Rept. RE-742, Grumman Corporate Research Center, Bethpage, NY, 1987, Appendix A.

[2]Katz, A., and Ross, A., "One on One Helicopter Combat Simulated by Chess Type Lookahead," *Journal of Aircraft*, Vol. 28, No. 2, 1991, pp. 158–160.

[3]Piercy, N. A. V., *Aerodynamics*, The English Universities Press, London, 1937, pp. 425–427.

[4]Munk, M., *Fundamentals of Fluid Dynamics for Aircraft Designers*, 1st ed., Ronald Press, New York, 1929, pp. 89–116.

[5]Glauert, H., "A General Theory of the Autogyro," ARC R&M 1111, Nov. 1926.

[6]Johnson, W., *Helicopter Theory*, Princeton Univ. Press, NJ, 1980.

[7]MDHC 86-48, "Performance and Range Report," Rept. 77-X-8011-3, Dec. 1986.

[8]Licher, R. M., and Toppel, B., "Longbow Apache Performance and Range Report," Document MSIP 00060-204, McDonnell Douglas Helicopter Co., Sept. 1990.

[9]Morris, P. M., Bender, G. L., Ottomeyer, J. D., Picasso, B. D., Higgins, L. B., and Savage, R., "Airworthiness and Flight Characteristics Test, Part 1, YAH-64 Attack Helicopter," Final Rept., USAAEFA Project 80-17-1, United States Army Aviation Engineering Flight Activity, Edwards Air Force Base, CA, Sept. 1981.